ADVANCED MATERIALS
www.advmat.de

MaterialsViews
www.MaterialsViews.com

Progress in Piezotronics and Piezo-Phototronics

*Zhong Lin Wang**

The fundamental principle of piezotronics and piezo-phototronics were introduced by Wang in 2007 and 2010, respectively. Due to the polarization of ions in a crystal that has non-central symmetry in materials such as the wurtzite structured ZnO, GaN and InN, a piezoelectric potential (*piezopotential*) is created in the crystal by applying a stress. Owing to the simultaneous possession of piezoelectricity and semiconductor properties, the piezopotential created in the crystal has a strong effect on the carrier transport at the interface/junction. *Piezotronics* is about the devices fabricated using the piezopotential as a "gate" voltage to tune/control charge carrier transport at a contact or junction. The *piezo-phototronic effect* is to use the piezopotential to control the carrier generation, transport, separation and/or recombination for improving the performance of optoelectronic devices, such as photon detector, solar cell and LED. This manuscript reviews the updated progress in the two new fields. A perspective is given about their potential applications in sensors, human-silicon technology interfacing, MEMS, nanorobotics and energy sciences.

1. Beyond Moore's Law with Diversity and Multi-Functionality

The Moore's law has been the roadmap that directs and drives the information technology in the last few decades. With the density of devices on a single silicon chip doubling every 18 months, increasing CPU speed and building a system on a chip are the major developing directions for IT technology (see the vertical axis in **Figure 1**). With the line width reaching close to 10 nm, a general question is how small a device can we fabricate at an industrial scale? What are the pros and cons with respect to stability and liability when devices get extraordinarily small? Is the speed the only driving parameter that we should look for? We know that the Moore's law will reach its limit one day, and it is just a matter of time. Then, the question is what should we look for beyond Moore's law?

Sensor networks and personal health care have been predicted as the major driving force for industries of the near future. As we have observed in today's electronic products, electronics are moving toward personal electronics, portable electronics, and polymer-based flexible electronics. We are looking for multifunctionality and diversity associated with electronics. Take a cell phone as an example, having a super fast computer in a cell phone may not be the major drive for the future market, but the consumers are looking for more functionality, such as health care sensors for blood pressure, body temperature and blood sugar level, interfacing with the environment with sensors for detecting gases, UV-radiation, and hazardous chemicals. In such a case, the IT technology is developing along another dimension, as presented in the horizontal axis in Figure 1. The near-future development of electronics is moving toward personal, portable, and polymer (flexible or organic) based electronics with the integration of multifunctional sensors and self-powering technology. A combination of CPU speed, density of memory and logic with the functionality tends to drive electronics toward smart systems and self-powered systems, which are believed to be the major roadmaps for electronics.

Once we interface humans with electronics, we inevitably have to consider human activities and the "signals" generated by a human, which are mostly mechanical actions and only a small portion of electrical signals. Electric signals transmitted by neuron systems have been studied for decades and various approaches have been developed to interface neuron signals with silicon-based technologies using field-effect transistors (lower part in Figure 1). Mechanical action, however, is not easy to be interfaced directly with silicon technologies without innovative design and approaches. The most conventional approach is to use sensors that are sensitive to strain variation (right-hand side in Figure 1). The signals from sensors can be detected and recorded by conventional electronics, which is so called passive detection, but these cannot to be used to control Si electronics. The current on-going research in flexible electronics is to minimize and eliminate the effect of strain introduced by the substrate on the performance of the electronic components built on a substrate, which can be termed as *passive* flexible electronics. On the other hand, we can utilize the deformation introduced by the substrate to induce electrical signals that can be used directly for controlling Si based electronics. A "mediator" or "translator" is needed to connect bio-mechanical action with the operation of silicon-based electronics. Piezotronics and piezo-phototronics were invented for such purposes, and they are considered *active* flexible electronics or bio-driven electronics.

The role anticipated to be played by piezotronics is similar to the mechanosensation in physiology.[1] Mechanosensation is

Prof. Z. L. Wang
School of Material Science and Engineering
Georgia Institute of Technology
Atlanta, Georgia 30332-0245 USA
E-mail: zlwang@gatech.edu

DOI: 10.1002/adma.201104365

 © 2012 WILEY-VCH Verlag GmbH & Co. KGaA, Weinheim

a response mechanism to mechanical stimuli. The physiological foundation for the senses of touch, hearing and balance, and pain is the conversion of mechanical stimuli into neuronal signals; the former is mechanical actuation and the latter is electrical stimulation. Mechanoreceptors of the skin are responsible for touch. Tiny cells in the inner ear are responsible for hearing and balance. Piezotronics was first introduced by Wang and co-workers in 2006 and 2007.[2–4] Piezo-phototronics was first coined in 2010.[5–7] Fundamental understanding about the effects and practical potential applications of the two fields has been demonstrated in the last few years. The basic principle of piezotronics and piezo-phototronics were reviewed in 2010.[8] In this paper, we will review the recent progress in afore-mentioned fields. Some in-depth understanding will be provided about their future applications.

Zhong Lin (ZL) Wang received his PhD from Arizona State University in physics. He now is the Hightower Chair in Materials Science and Engineering, Regents' Professor, Engineering Distinguished Professor and Director, Center for Nanostructure Characterization, at Georgia Tech. Dr. Wang has made original and innovative contributions to the synthesis, discovery, characterization and understanding of fundamental physical properties of oxide nanobelts and nanowires, as well as applications of nanowires in energy sciences, electronics, optoelectronics and biological science. His discovery and breakthroughs in developing nanogenerators establish the principle and technological road map for harvesting mechanical energy from environment and biological systems for powering a personal electronics. His research on self-powered nanosystems has inspired the worldwide effort in academia and industry for studying energy for micro-nano-systems. He coined and pioneered the field of piezotronics and piezo-phototronics by introducing piezoelectric potential gated charge transport process in fabricating new electronic and optoelectronic devices for smart MEMS, active flexible electronics, sensors and human-Si CMOS interfacing. Details can be found at: http://www.nanoscience.gatech.edu

2. Piezopotential – The Core of Piezotronics and Piezo-Phototronics

Silicon-based CMOS technology is operated by an electrically driven charge-transport process. To control the operation of CMOS directly by mechanical action, one must find an electric signal that can be generated as a result of mechanical action. The most obvious choice is piezoelectricity. For this purpose, we choose wurtzite materials, such as ZnO, GaN, InN and ZnS, which simultaneously have piezoelectric and semiconductor properties. ZnO, for example, has a non-central symmetric crystal structure, which naturally produces a piezoelectric effect once the material is strained. A wurtzite crystal has a hexagonal structure with a large anisotropic property in the *c*-axis direction and perpendicular to the *c*-axis. Simply, the Zn^{2+} cations and O^{2-} anions are tetrahedrally coordinated and the centers of the positive ions and negatives ions overlap with each other. If stress is applied at an apex of the tetrahedron, the center of the cations and the center of anions are relatively displaced, resulting in a dipole moment (**Figure 2**a). A constructive add-up of the dipole moments created by all units in the crystal creates a piezoelectric field, which results in a macroscopic potential drop along the straining direction in the crystal. This is the piezoelectric potential (*piezopotential*) (Figure 2b).[9] The piezopotential can serve as the driving force for the flow of electrons in the external load once subjected to mechanical deformation, which is the fundamental working principle of a nanogenerator.[10–13]

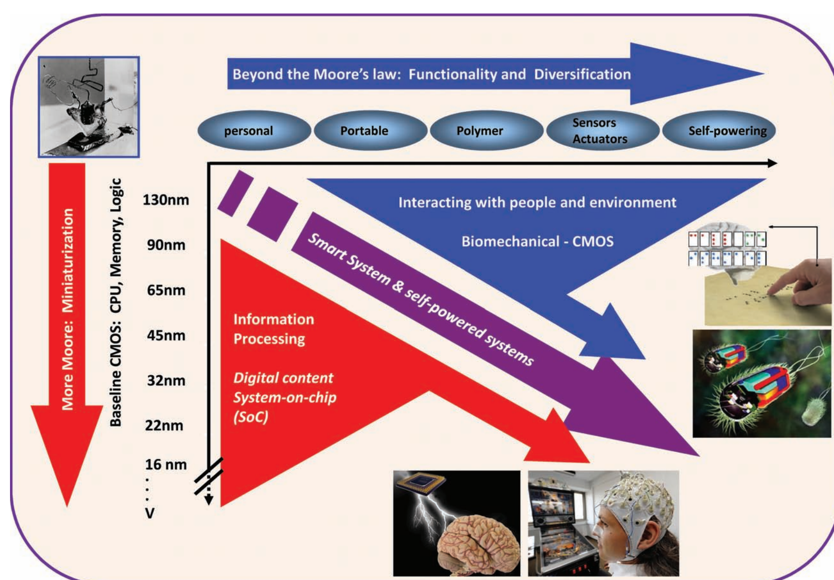

Figure 1. Future perspective of electronics beyond the Moore's law. The vertical axis represents a miniaturization and increase of device density, CPU speed and memory. The horizontal axis represents the diversity and functionality for personal and portable electronics. The future of electronics is an integration of CPU speed and functionality. It is anticipated that an integration of mechanical action through piezotronics in electronic systems is an important aspect of interfacing human and CMOS technologies.

The distribution of a piezopotential in a *c*-axis ZnO nanowire (NW) has been calculated using the Lippman theory[14–16] without considering the doping in ZnO. For a NW with a length of 1200 nm and a hexagonal side length of 100 nm, a tensile force of 85 nN creates a potential drop of approximately 0.4 V between the two ends, with the +c side positive (the right-hand side in

© 2012 WILEY-VCH Verlag GmbH & Co. KGaA, Weinheim

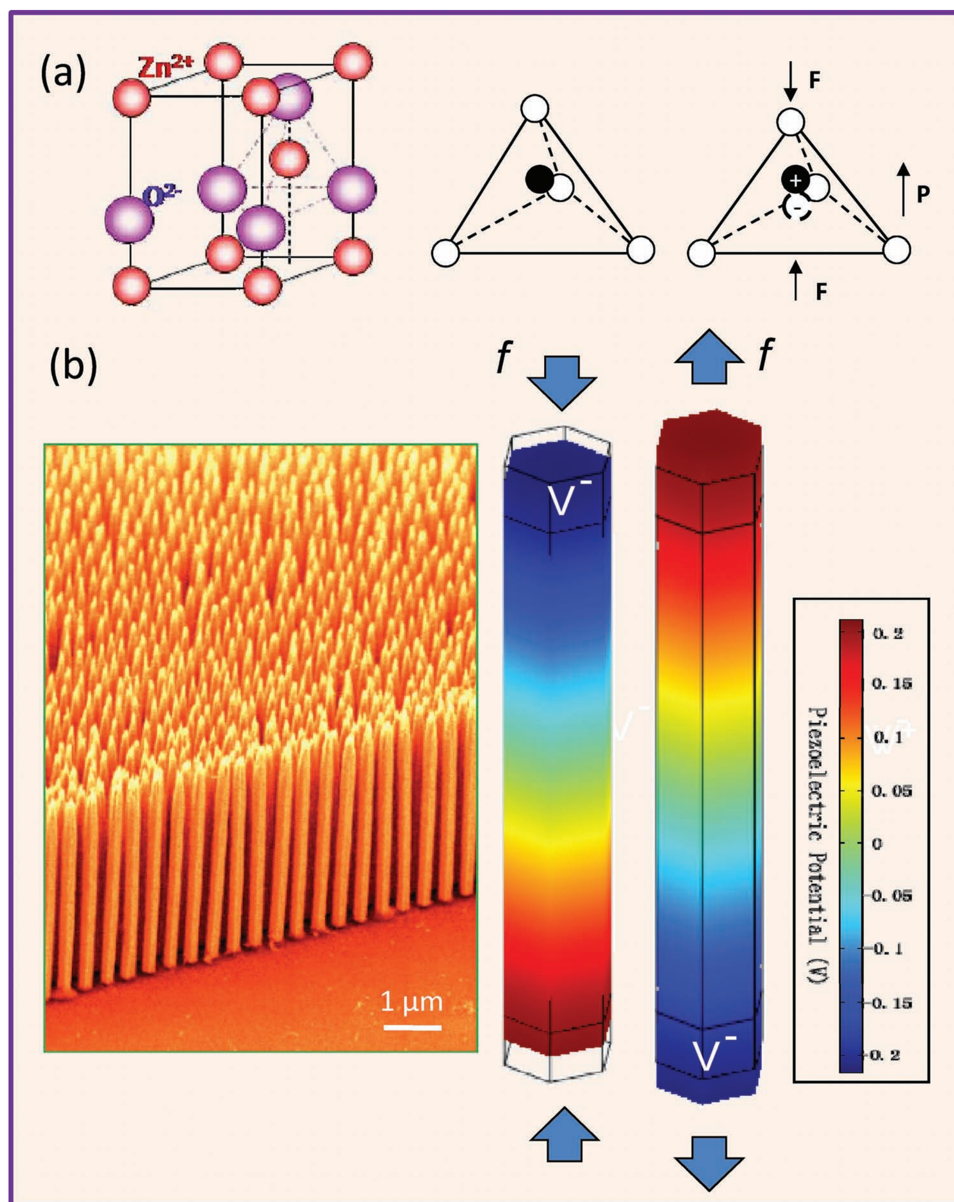

Figure 2. Piezopotential in wurtzite crystal. (a) Atomic model of the wurtzite-structured ZnO. (b) Aligned ZnO nanowire arrays by solution based approach. Numerical calculated distribution of piezoelectric potential along a ZnO NW under axial strain. The growth direction of the NW is *c*-axis. The dimensions of the NW are L = 600 nm and a = 25 nm; the external force is f_y = 80 nN Reproduced with permission.[15] Copyright 2009. AIP.

Figure 2b).[17] When the applied force changes to a compressive strain, the piezoelectric potential reverses with the potential difference remaining 0.4 V but with the –*c*-axis side at a higher potential. The creation of this inner crystal potential is the core of piezotronics.

3. Materials System for Piezotronics and Piezo-Phototronics

One-dimensional nanomaterials, such as nanowires and nanobelts, are ideal for piezotronics and piezo-phototronics, because they can tolerate a large mechanical strain. ZnO, GaN, InN and possibly doped PZT materials are potential candidate for piezotronics. Currently, the most popular structure is ZnO nanowires (NWs) for three main reasons. First, ZnO NWs can be easily grown in large quantities using a vapor-solid process or chemical approach at low temperature. Secondly, they are biologically compatible and environmentally friendly. Finally, they can be grown on a substrate and any shape of substrate. The vapor-solid growth usually takes place in a tube furnace by vaporizing ZnO powders in the presence of carbon at a temperature of ~900 °C. Patterned growth is possible with the introduction of a Au catalyst. Pulse laser deposition (PLD) can be

 © 2012 WILEY-VCH Verlag GmbH & Co. KGaA, Weinheim

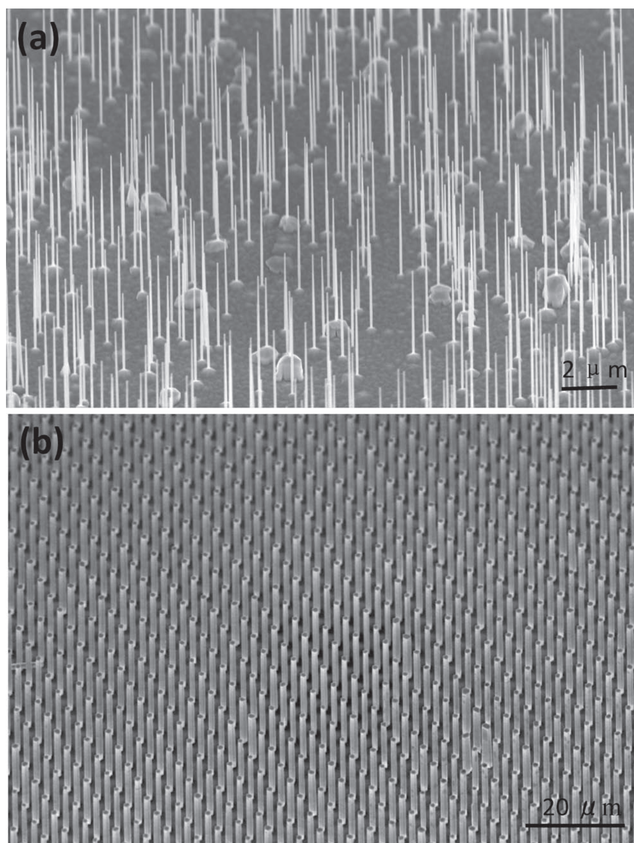

Figure 3. ZnO nanowire arrays grown by (a) pulse laser deposition technique and (b) low-temperature solution-based approach. Panels (a) and (b) reproduced with permission.[18,21] Copyright ACS, 2010/2009.

used for NW growth. A KrF excimer laser (248 nm) was used as the ablation source to focus on a ceramic target, which is a stack of ZnO powder. Control of the pressure can give a nice NW array (**Figure 3**a).[18]

The most commonly used chemical agents for the hydrothermal synthesis of ZnO NWs are zinc nitrate hexahydrate and hexamethylenetetramine.[19,20] Zinc nitrate hexahydrate salt provides Zn^{2+} ions required for building up ZnO NWs. Water molecules in the solution provide O^{2-} ions. Even though the exact function of hexamethylenetetramine during the ZnO NW growth is still unclear, it is believed to act as a weak base, which would slowly hydrolyze in the water solution and gradually produce OH^-. This is critical in the synthesis process because the Zn2+ ions in solution would precipitate very quickly in the high pH environment if the hexamethylenetetramine hydrolyzes very fast and produces a lot of OH^- in a short period of time. Using a pattern generated by laser interference, well-aligned NW arrays have been grown at a temperature of around 85 °C (Figure 3b).[21]

NWs grown by the vapor-phase technique at high temperature usually have low defects and they are most adequate for studying piezotronic and piezo-phototronic effects.[22,23] A treatment in an oxygen plasmon can effectively reduce the vacancy concentration. The low-temperature chemically grown NWs have a relatively high concentration of defects, and they are most useful for piezoelectric nanogenerators.

4. Piezotronics

4.1. Piezotronic Transistors

In order to illustrate the basic concept of piezotronics, we first start from a traditional metal oxide semiconductor field-effect transistor (MOS FET). For an n-channel MOS FET (**Figure 4**a), the two n-type doped regions are the drain and source; a thin insulator oxide layer is deposited on the p-type region to serve as the gate oxide, on which a metal contact is made as the gate. The current flowing from the drain to source under an applied external voltage V_{DS} is controlled by the gate voltage V_G, which controls the channel width for transporting the charge carriers. In analogy, for a single channel FET fabricated using a semiconductor NW (Figure 4b), the drain and source are the two metal electrodes at the two ends, and a gate voltage is applied at the top of the NW or through the base substrate.

A piezotronic transistor is a metal–NW–metal structure, such as Au-ZnO-Au or Ag-ZnO-Ag, as schematically shown in Figure 4(c) and (d) once strain is applied through the substrate.[24] The fundamental principle of the piezotronic transistor is to control the carrier transport at the M-S interface through tuning at the local contact by creating a piezopotential at the interface region in the semiconductor by applying strain. This structure is different from the CMOS design as follows. First, the externally applied gate voltage is replaced by an inner crystal potential generated by the piezoelectric effect, thus, the "gate" electrode is eliminated. This means that the piezotronic transistor only has two leads: drain and source. Secondly, the control over the channel width is replaced by a control at the interface. Since the current transported across a M-S interface is the exponential of the local barrier height at the reversely biased case, the ON and OFF ratio can be rather high due to the non-linear effect. Finally, a voltage-controlled device is replaced by an external strain/stress controlled device, which is likely to have complimentary applications to CMOS devices.

When a ZnO NW device is under strain, there are two typical effects that may affect the carrier transport process. One is the piezoresistance effect[25,26] because of the change in bandgap, charge carrier density and possibly density of states in the conduction band of the semiconductor crystal under strain. This effect is a symmetric effect on the two end contacts and has no polarity, which will not produce the function of a transistor. Piezoresistance is a common feature of any semiconductors, such as Si and GaAs, and is not limited to the wurtzite family. The other is the piezoelectric effect because of the polarization of ions in a crystal that has non-central symmetry, which has an asymmetric or non-symmetric effect on the local contacts at the source and drain owing to the polarity of the piezopotential. In general, the negative piezopotential side raises the barrier height at the local contact of metal n-type semiconductor, possibly changing a Ohmic contact to Schottky contact, a Schottky contact to "insulator" contact; while the positive piezopotential side lowers the local barrier height, changing a Schottky contact to an Ohmic contact. But the degree of changes in the barrier heights depends on the doping type and doping density in the NW. The piezoelectric charges are located at the ends of the wire, thus they directly affect the local contacts. The piezotronic

 © 2012 WILEY-VCH Verlag GmbH & Co. KGaA, Weinheim

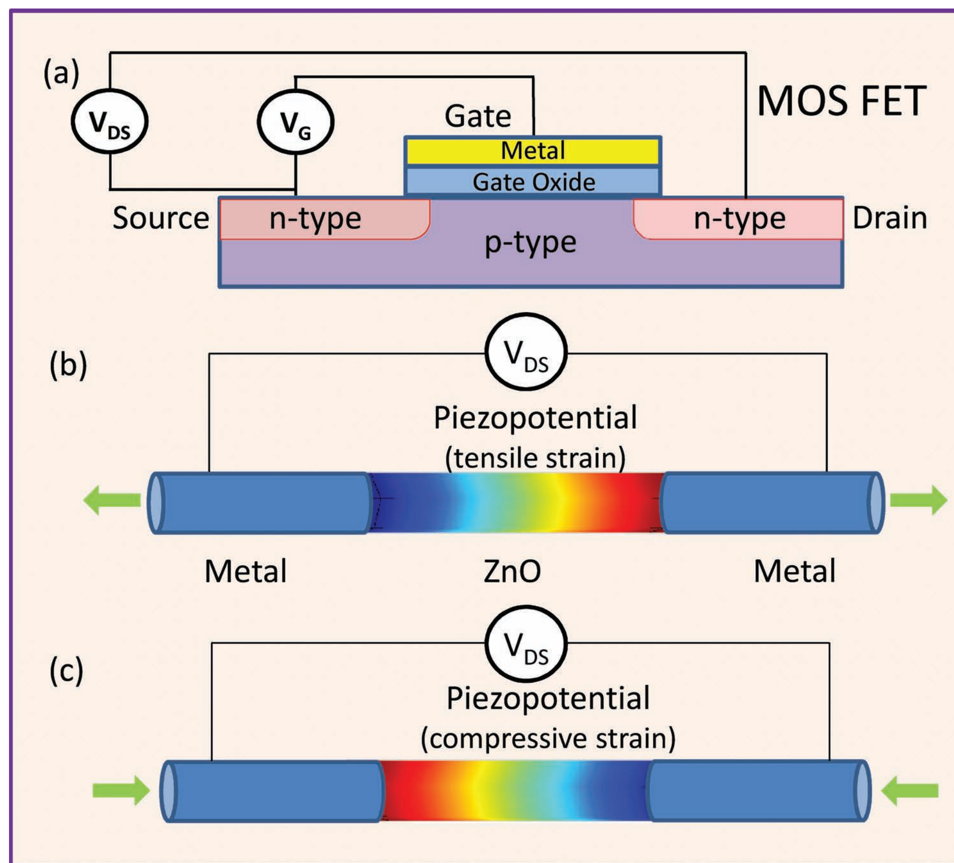

Figure 4. Schematic of (a) an n-channel MOS FET and (b) a semiconductor nanowire FET; Schematic of a piezotronic transistor with tensile strain (c nd compressive strain (d), where the gate voltage that controls the channel width is replaced by a piezopotential that controls the transport across the metal-semiconductor interface.

effect is likely limited to the wurtzite family such as ZnO, GaN, CdS and InN. It is important to point out that the polarity of the piezopotential can be switched by changing tensile strain to compressive strain. Thus, the device can be changed from a control at source to a control at drain simply by reversing the sign of strain applied to the device.

4.2. Effect of Piezopotential on Metal-Semiconductor Contact

When a metal and a n-type semiconductor form a contact, a Schottky barrier (SB) ($e\varphi_{SB}$) is created at the interface if the work function of the metal is appreciably larger than the electron affinity of the semiconductor (**Figure 5**a). Current can only pass through this barrier if the applied external voltage is larger than a threshold value (φ_i) and its polarity is positive at the metal side (for an n-type semiconductor). If a photon excitation is applied at the interface, the newly generated electrons in the conduction band tend to move away from the contact, while the holes tend to move close to the interface toward the metal side. The accumulated holes at the interface modify the local potential profile, so that the effective height of the Schottky barrier is lowered (Figure 5b), which increases the conductance.

Once a strain is created in a semiconductor that also has piezoelectric property, a negative piezopotential at the semiconductor side effectively increases the local SB height to $e\varphi$ (Figure 5c), while a positive piezopotential reduces the barrier height. The role played by the piezopotential is to change the local contact characteristics effectively through an internal field depending on the crystallographic orientation of the material and the sign of the strain, thus, the charge carrier transport process is tuned/gated at the metal–semiconductor (M–S) contact. By considering the change in piezopotential polarity by switching the strain from tensile to compressive, the local contact characteristics can be tuned and controlled by the magnitude of the strain and the sign of strain.[27,15] Therefore, the charge transport across the interface can be largely dictated by the created piezopotential, which is the gate effect. This is the core of piezotronics.

On the other hand, if we excite a MS contact by photons that have an energy larger than the bandgap of the semiconductor, electron-hole pairs are generated at the vicinity of the contact. The presence of free-carriers at the interface can effectively reduce the Schottky barrier height. Therefore, piezopotential can increase the local barrier height, while laser excitation can effectively reduce the local barrier height. The two effects can be applied in a complimentary way for controlling the charge

© 2012 WILEY-VCH Verlag GmbH & Co. KGaA, Weinheim

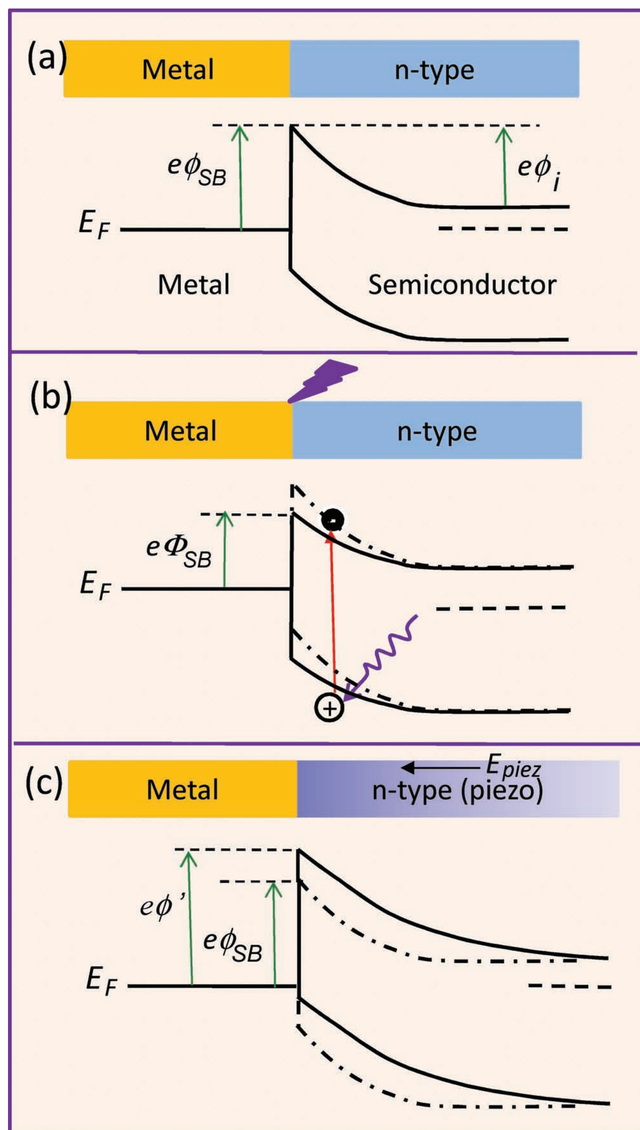

Figure 5. Energy band diagram for illustrating the effects of laser excitation and piezoelectricity on a Schottky contacted metal-semiconductor interface. (a) Band diagram at a Schottky contacted metal-semiconductor interface. (b) Band diagram at a Schottky contact after exciting by a laser that has a photon energy higher than the bandgap, which is equivalent to a reduction in the Schottky barrier height. (c) Band diagram at the Schottky contact after applying a strain in the semiconductor. The piezopotential created in the semiconductor has a polarity with the end in contacting with the metal being low.

transport at the interface. This is a coupling between piezoelectricity and photon excitation.[5]

4.3. Effect of the Piezopotential on a p-n Junction

When p-type and a n-type semiconductors form a junction, the holes at the p-type side and the electrons at the n-type side tend to redistribute to balance the local potential, the interdiffusion and recombination of the electrons and holes in the junction region forms a charge depletion zone. The presence of such a carrier free zone can significantly enhance the piezoelectric effect, because the piezo-charges will be mostly preserved without being screened by local residual free carriers. As shown in **Figure 6**a, for a case that the p-type side is piezoelectric and a strain is applied, local net negative piezo-charges are preserved at the junction provided the doping is relatively low so that the local free carriers are not enough to screen the piezo-charges completely. The piezopotential tends to raise the local band slightly and introduce a slow slope to the band structure.[8] Alternatively, if the applied strain is switched in sign (Figure 6b), the positive piezo-charges at the interface creates a dip in the local band. A modification in the local band may be effective for trapping the holes so that the electron-hole recombination rate can be largely enhanced, which is very beneficial for improving the efficiency of an LED. Furthermore, the inclined band tends to change the mobility of the carriers moving toward the junction.

By the same token, if the n-type side is piezoelectric, similar band structure change can be induced from the piezoelectric effect, as shown in Figures 6(c, d). The band structure modification at the interface/junction by piezoelectric charges introduces some fundamental changes to the local band structure, which is effective for controlling the device performance.

For a p-n junction made of two materials with distinctly different bandgaps, local piezo-charges can also significantly affect the band profile, as shown in **Figure 7**, so that the transport of the charge carriers across the interface will be significantly modified. Take the case shown in Figure 7e as an example, the barrier height at the interface as created by band misalignment can be reduced so that the electrons can be effectively transported across the interface. While for the case of Figure 7f, the height and width of the barrier at the interface are increased by piezo charges. As for the case presented in Figure 7b, the local trapping of holes can be significantly increased, which may be beneficial for LED. But for the case in Figure 7a, it may have negative effect on LED efficiency. Therefore, the presence of piezo charges at the junction can be useful for some optoelectronic processes.

4.4. Piezotronic Transistor and Logic Calculation

A piezotronic transistor is made of a single ZnO NW with its two ends, which are the source and drain electrodes, being fixed by silver paste on a polymer substrate (**Figure 8**A). Once the substrate is bent, a tensile/compressive strain is created in the NW since the mechanical behavior of the entire structure is determined by the substrate. Utilizing the piezopotential created inside the NW, the gate input for a NW strain-gated transistor (SGT) is an externally-applied strain rather than an electrical signal.[28] I_{DS}–V_{DS} characteristic for each single ZnO-NW SGT is obtained as a function of the strain created in the SGT (Figure 8A) before further assembly into logic devices. A NW SGT is defined as forward biased if the applied bias is connected to the drain electrode (Figure 8A). For a SGT, the external mechanical perturbation induced strain (ε_g) acts as the gate input for controlling the "on"/"off" state of the NW SGT. The positive/negative

© 2012 WILEY-VCH Verlag GmbH & Co. KGaA, Weinheim

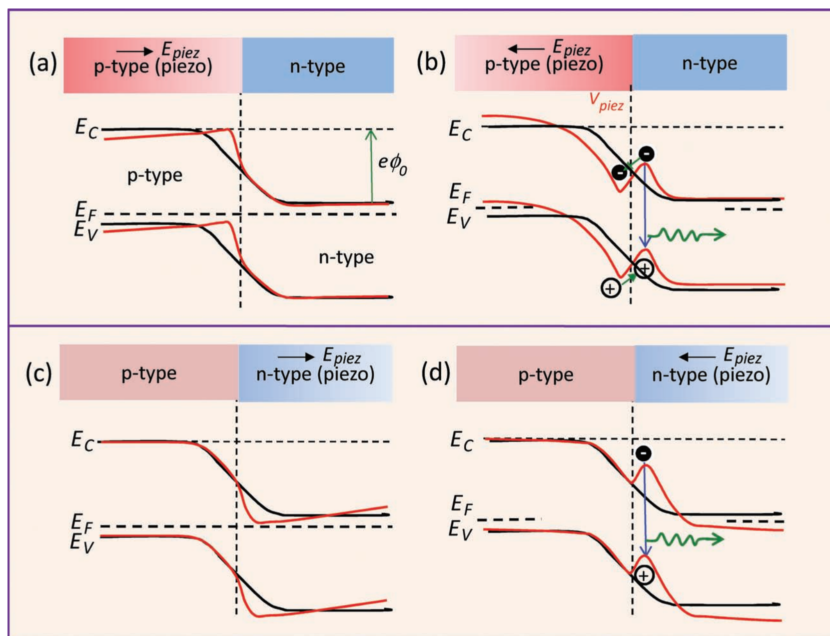

Figure 6. Energy band diagram for illustrating the effect of piezoelectricity on a *pn* junction that is made of two materials of similar bandgaps. The band diagrams for the *pn* junction with and without the presence of piezoelectric effect for the four possible cases are shown using dark and red curves, respectively. The bandgap for the n-type and p-type are assumed to be about equal. The effect of reversal in polarity is presented.

strain is created when the NW is stretched/compressed. The SGT behaves in a similar way to a n-channel enhancement-mode MOSFET, apparently indicating the working principle of the SGT.

The working principle of a piezotronic transistor is illustrated by the band structure of the device.[31] A strain free ZnO NW may have Schottky contacts at the two ends with the source and drain electrodes but with different barrier heights of Φ_S and Φ_D, respectively (Figure 8B-a). When the drain is forward biased, the quasi-Fermi levels at the source ($E_{F,S}$) and drain ($E_{F,D}$) are different by the value of eV_{bias}, where V_{bias} is the applied bias (Figure 8B-b). An externally applied mechanical strain (ε_g) results in both band structure change and piezoelectric potential field in a ZnO NW. The former leads to the piezoresistance effect, a red shift in local photoluminescence[29] and an enhanced photocurrent,[30] which is a non-polar and symmetric effect at the both source and drain contacts. Since ZnO is a polar structure along c-axis, straining in axial direction (c-axis) creates a polarization of cations and anions in the NW growth direction, resulting in a piezopotential drop from V^+ to V^- along the NW, which produces an asymmetric effect on the changes in the SB heights (SBHs) at the drain and source electrodes. Under tensile strain, the SBH at the source side reduces, resulting in increased I_{DS}. For the compressively strained piezotronic transistor, the sign of the piezopotential is reversed, thus the SBH at the source side is raised (Figure 8B-d), resulting in a large decrease in I_{DS}. Therefore, as the strain ε_g is swept from compressive to tensile regions, the I_{DS} current can be effectively turned from "on" to "off" while V_{DS} remains constant. This is the fundamental principle of the piezotronic transistor.

Based on the piezotronic transistor described above, universal logic operations such as inverters, NAND, NOR, XOR gates have been demonstrated for performing piezotronic logic calculations,[31] which have the potential to be integrated with the MEMS technology for achieving advanced and complex functional actions. The key difference between the logic operations using piezotronics from the CMOS logic units is that the piezotronic logic is driven and controlled by strain/deformation, with applications in human-CMOS interfacing.

4.5. Piezotronic Memory

The external mechanical perturbation induced strain (ε_g) acts as the programming input for modulating the hysteretic *I–V* characteristics of the piezoelectrically modulated resistive memory (PRM) cell.[31] A positive/negative strain is created when the ZnO NW is stretched/compressed (see Supporting Information for calculation of the strain in the PRM cell). Interesting phenomena was observed when a PRM cell experienced straining (**Figure 9**a). When the PRM cell was tensile stretched (ε = 1.17%), the hysteretic switching curve shifted towards lower voltage side by 1.49 V (red line in Figure 9a); when the cell was compressively deformed (ε = –0.76%), the hysteretic switching curve shifted towards higher voltage side by 1.18 V (blue line in Figure 9a). $V_{th,S+}$, $V_{th,S0}$, $V_{th,S-}$ and $V_{th,D+}$, $V_{th,D0}$, $V_{th,D-}$ are the threshold switching voltages for the PRM cell with tensile, zero and compressive strains, respectively. The ratios of conductance between LRS and HRS for the PRM cell remain steady at high values (~10^5) under different strains, demonstrating the stable performance of the cell and its potential feasibility for applications in flexible memory and logic operations. The intrinsic rectifying behavior of the PRM cell may solve the sneak path problem as well as reduce the static power consumption, which allows for construction of large passive resistive-switching device arrays. The changes in threshold switching voltages of the PRM cell with different strains have been plotted in Figure 9b. It can be seen that the change in both the $V_{th,S}$ and $V_{th,D}$ almost linearly depends on strain applied to the PRM cell, while the width of the HRS window ($V_{th,Si}$ - $V_{th,Di}$, where i = +, 0, –) remains almost constant for different strain values.

The modulation effect of strain on the hysteric switching behavior of the PRM cell can then be understood and explained using the band-diagram of the working device (Figure 9c). If the PRM cell is under tensile strain with the Schottky barrier at drain side being forward-biased (V > 0 in Figure 9a), the positive piezoelectric potential resulting from the positive strain-induced polarization charges reduced the SBH at the reverse-biased source barrier; while the negative piezoelectric potential resulting from the negative strain-induced polarization charges increased the SBH at the forward-biased drain

© 2012 WILEY-VCH Verlag GmbH & Co. KGaA, Weinheim

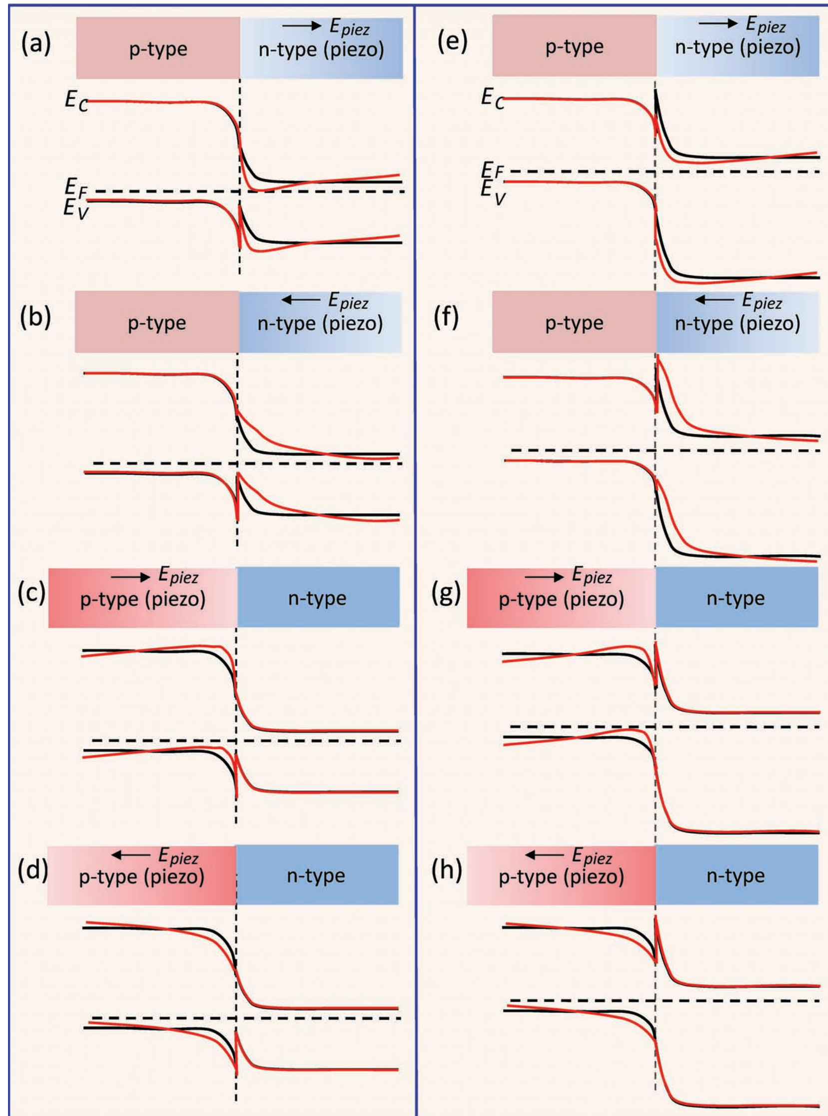

Figure 7. Energy band diagram for illustrating the effect of piezoelectricity on a heterostructured *pn* junction. The band diagrams for the *pn* junction with and without the presence of piezoelectric effect for the eight possible cases are shown using dark and red curves, respectively. The effect of reversal in polarity is also presented.

barrier (red line in Figure 9c). Since the *I–V* characteristic in this situation is dictated by the reversely-biased source barrier, the existence of strain-induced piezoelectric potential results in the shift of switching threshold voltage from $V_{th,S0}$ to $V_{th,S+}$, indicating only a smaller bias is required to switch the PRM cell from HRS to LRS state. Alternatively, if the Schottky barrier at drain side is reverse-biased ($V < 0$ in Figure 9a), the SBH is still reduced at the source barrier while it is increased at the drain barrier (Figure 9b) since the polarity of the strain did not change, and hence the piezoelectric potential remained negative and positive at source and drain barriers, respectively. The *I–V* characteristic is now dictated by the reversely-biased drain side in this case, and a shift of switching threshold voltage from $V_{th,D0}$ to $V_{th,D+}$ was observed, indicating a larger bias has to be applied in order to switch the PRM cell from HRS to LRS state. By the same token, in the case of applying a compressive strain to the PRM cell, the shift of switching threshold voltage from $V_{th,S0}$ to $V_{th,S_}$ and $V_{th,D0}$ to $V_{th,D_}$ can be explained. Therefore, a measure of V_{th} directly provides a measure of the applied strain if the system is properly calibrated. This is the fundamental mechanism for fabricating strain memory unit.[31]

4.6. Basic Theory of Piezotronic Transistor

We have developed the theoretical frame of piezotronics by studying the charge transport across metal-semiconductor contact and p-n junction with the introduction of piezopotential.[24] Besides numerical calculations, we have also derived analytical solutions under simplified conditions, which are useful for illustrating the major physical pictures of the piezotronic devices. As for a metal-semiconductor contact, the transported current density under an applied field V is given be:

$$J_n \approx J_{D0} \exp\left(\frac{q^2 \rho_{piezo} W_{piezo}^2}{2\varepsilon_s kT}\right)\left[\exp\left(\frac{qV}{kT}\right) - 1\right] \quad (1)$$

where ρ_{piezo} (x) is density of polarization charges, W_{piezo} is the width of the distribution zone of the piezo charges at the interface, ε_S is the relative dielectric constant. This means that the current transported across the M-S contact is an exponential function of the local piezo-charges, the sign of which depends on the strain. Therefore, the current to be transported can be effectively tuned or controlled by not only the magnitude of the strain, but also by the sign of the strain (tensile vs compressive). This is the mechanism of the piezotronic transistor for M-S case.

Alternatively, for wurtzite NWs with *c*-axis growth direction, the current density is:

$$J = J_{D0} \exp\left(\frac{q e_{33} s_{33} W_{piezo}}{2\varepsilon_s kT}\right)\left[\exp\left(\frac{qV}{kT}\right) - 1\right] \quad (2)$$

where the axial strain is s_{33} and is e_{33} is the piezocoefficient. It is clear that the current transported across the M-S interface is directly related to the exponential of the local strain, which means that the current can tuned on or off by controlling strain.

5. Piezo-Phototronics

Based on the analysis in Figures 6 and 7, the presence of the localized piezoelectric charges at the junction can significantly affect the behavior of the charge carriers and the corresponding optoelectronic properties. This is the piezo-phototronic effect, which is about the consequence of piezopotential on the generation, transport, separation and/or recombination of

© 2012 WILEY-VCH Verlag GmbH & Co. KGaA, Weinheim

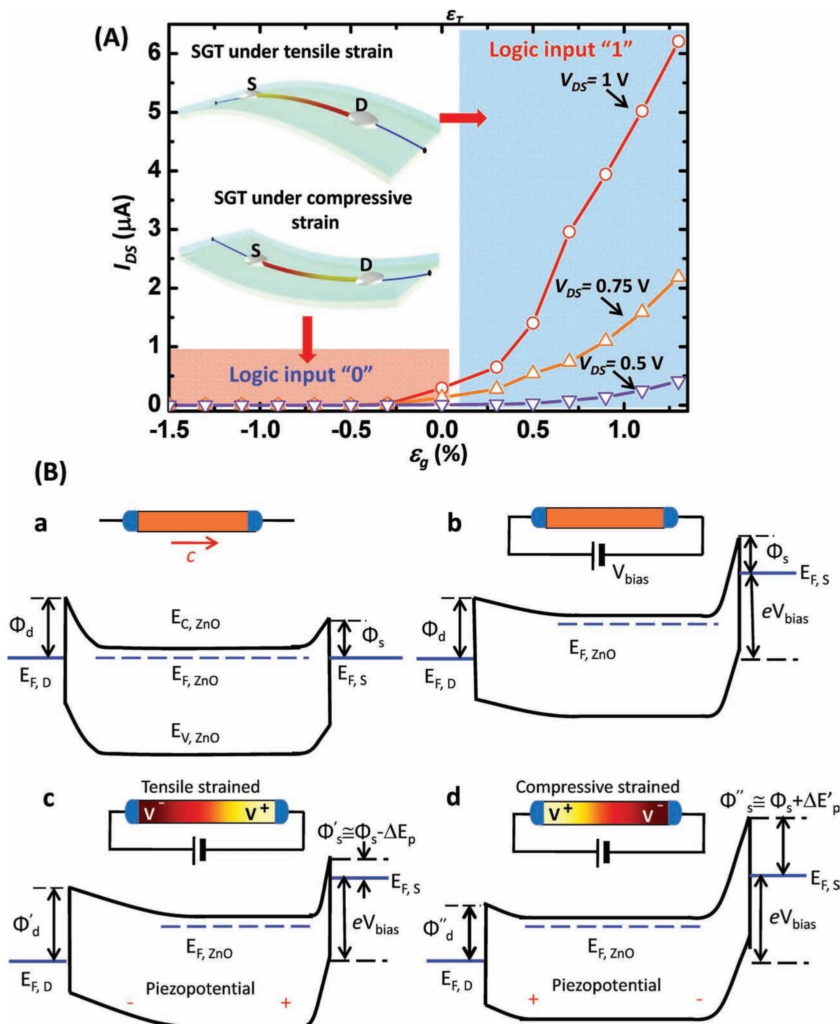

Figure 8. Strain-gated transistor (SGT). (A) Current–strain ($I_{DS} - \varepsilon_g$) transfer characteristic for a ZnO SGT device with strain sweeping from ε_g = -0.53% to 1.31% at a step of 0.2%, where the V_{DS} bias values were 1 V, 0.75 V and 0.5 V, respectively. (B) The band structures of the ZnO NW SGT under different conditions for illustrating the mechanism of SGT. The crystallographic *c*-axis of the nanowire directs from drain to source. (a) The band structure of a strain-free ZnO NW SGT at equilibrium with different barrier heights of Φ_S and Φ_D at the source and drain electrodes, respectively. (b) The quasi-Fermi levels at the source ($E_{F,S}$) and drain ($E_{F,D}$) of the ZnO SGT are split by the applied bias voltage V_{bias}. (c) With tensile strain applied, the SBH at the source side is reduced from Φ_S to $\Phi'_S \cong \Phi_S - \Delta E_P$. (d) With compressive strain applied, the SBH at the source side is raised from Φ_S to $\Phi''_S \cong \Phi_S + \Delta E'_P$ .. Reproduced with permission.[28] Copyright ACS, 2011.

charge carriers at the junction, and is a three way coupling among piezoelectricity, semiconductor behavior and photon excitation. We now use three examples to illustrate the piezo-phototronic effect on solar cell, photodetector and LED.

5.1. Piezo-Phototronic Effect on Solar Cell

5.1.1. Piezopotential on Output Potential

A solar cell is a process of photon-generated charges, in which the charge separation is critical for the conversion efficiency. Once an electron-hole pair is generated at a p-n junction by photon excitation, the electron tends to move in the n-side away from the junction, while the hole moves into the p-side. Owing to the Coulomb attraction between the electron and hole, they tend to recombine, resulting in a lower efficiency. If the energy required for the charge separation is too high, the electron and hole cannot be effectively separated. If the energy required is too low, the electron and hole interaction tend to make them recombine. Either of the processes are not beneficial for a high output solar cell. Therefore, using the modification of the piezopotential to the p-n junction, we probably can optimize the band structure at the interface so that the charges can be effectively separated.[32]

We now use a solar cell based on ZnO-P3HT as an example to illustrate the piezo-phototronic effect on the output.[33] A schematic of the device is shown in **Figure 10**a. Long ZnO microwires were chosen because they are easy to manipulate. To avoid the movement of ZnO wire in the electromechanical measurement process, the bottom at one end of the ZnO wire was fixed by a thin epoxy paint film on the PS substrate under optical microscopy. The P3HT in C6H5Cl solution was then dropped on the fixed end of the ZnO wire to produce the p-n heterojunction. The ZnO wire was not completely covered by the P3HT. The other end of the ZnO wire was fixed by silver paste, serving as an electrode. Figure 10b shows an optical image of a fabricated device, showing that a smooth ZnO wire was connected by P3HT and silver paste on the substrate. The used ZnO micro/nanowires have a wurtzite structure and grow along the [0001] direction by the TEM analysis, as shown in Figure 10c. The short-circuit current I_{sc} and V_{oc} under the different strains are shown in Figure 10d and e. The V_{oc} increases and decreases with increasing the compressive and tensile strains, respectively. However, the I_{sc} almost shows a constant value of 0.035 nA under the different strains.

We calculated the distribution of piezopotential in a single ZnO wire with a growth direction of [0001] by using the Lippman theory, as shown in **Figure 11**. For simplicity of the calculation, we ignore the doping in ZnO so that it is assumed to be an insulator. The diameter and length of ZnO wire are 1 and 10 μm, respectively. The tensile and compressive strains are 0.1% and –0.1%, respectively. When the ZnO wire was stretched along the c-axial direction, it can create a polarization of cations and anions along the c-axial direction and result in a piezopotential change from V_- to V_+ along the ZnO wire, as shown in Figure 11a. On the basis of the above discussions and calculation of piezopotential, the modulation effect of the strain

© 2012 WILEY-VCH Verlag GmbH & Co. KGaA, Weinheim

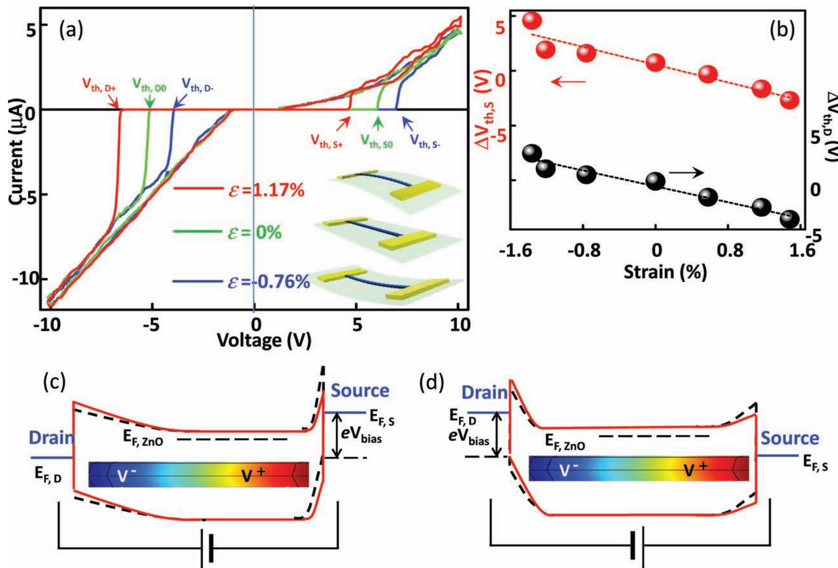

Figure 9. Stain-modulated hysteretic switching of piezoelectrically modulated resistive memory (PRM) cell. (a) *I–V* characteristics of ZnO PRM cells under tensile, zero and compressive strains respectively. (b) Dependence of threshold voltages on applied strains. Both $V_{th,S}$ (in red) and $V_{th,D}$ (in black) almost linearly depends on strain applied to the PRM cell, while the width of the HRS window remains almost constant for different strain values. (c) Schematic of band-diagram of PRM cell under tensile strain. Red solid lines represent band-diagrams after tensile strain is applied. Black dashed lines represent band-diagrams under strain free condition. The color gradient represents the distribution of piezopotential field. Reproduced with permission.[31] Copyright ACS, 2011.

on the V_{oc} of the fabricated device, as shown in Figures 10a, can then be understood and explained by using the band-diagram of the P3HT/ZnO heterojunction at the interface. We can build the following model for understanding our measured results. When the device of the [0001] type is under the tensile strain (Figure 11a), the negative piezopotential is in contact with the P3HT. The negative piezoelectric polarization charges at the interface lift the local conduction band level of ZnO, which can result in a decrease of ΔE and V_{oc} (ΔE – as shown in Figure 11a). Moreover, for the cases in Figures 11b, the positive piezoelectric polarization charges at the interface can lower the local conduction band level of ZnO, resulting in an increase of ΔE and V_{oc} (ΔE^+as shown in Figure 11b).

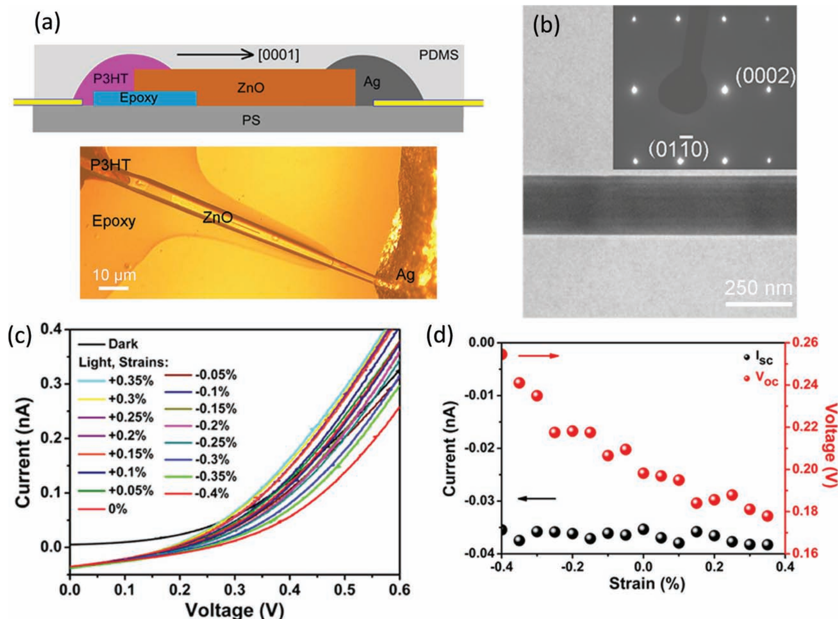

Figure 10. (a) Schematic of a fabricated device of the [0001] type. (b) Optical image of the fabricated device. (c) A TEM image of a single ZnO nanowire and the corresponding selected area electron diffraction (SAED) pattern. (d) *I–V* characteristics of the device under different strain. (e) Dependence of short-circuit current I_{sc} and the open-circuit voltage V_{sc} on applied strain. Reproduced with permission.[33] Copyright ACS, 2011.

5.1.2. Piezopotential on Charge Separation in Heterostructured Core-Shell Nanowire Solar Cell

Epitaxial core-shell NWs grown with different materials acquire in general elastic strain as a result of a misfit between the inherent crystal lattices of the core and shell materials. Such a static and internally built strain can create piezoelectric polarization in the NW. Xu an co-workers has theoretically investigated the piezopotential created in a core-shell NW as a result of intrinsic strain[34,35] and its possibility for high-efficient solar cell.[36] A model system is a III–V zinc blende (ZB) NWs grown along the [111] direction and III–V wurtzite (WZ) NWs grown along the [0001] direction. The lattice-mismatch-induced strain in an epitaxial core-shell nanowire gives rise to an internal electric field along the axis of the nanowire. This piezoelectric field results predominantly from atomic layer displacements along the nanowire axis within both the core and shell materials and can appear in both zinc blende and wurtzite crystalline core-shell nanowires. The effect can be employed to separate photon-generated electron-hole pairs in the core-shell nanowires and thus offers a new device concept for solar energy conversion. In comparison with previously proposed NW photovoltaic devices, this design does not require the fabrication of a p-n junction in the NWs, which leads to a technology advantage in the device fabrication. Nevertheless, the axial p-n junctions could be integrated into the core-shell NWs to achieve enhancement of solar energy conversion. Such a theoretical prediction remains to be verified by experiments.

Recently, Zheng and Woo have theoretically studied the possibility of using the spontaneous polarization in ferroeledtric nanorods for enhancing photovoltaic effect.[37] The materials they have analyzed are based on traditional piezoelectric crystals, such as PZT and $BaTiO_3$. Taking into account the polarization charge screening in the electrodes and near-surface inhomogeneous polarization

© 2012 WILEY-VCH Verlag GmbH & Co. KGaA, Weinheim

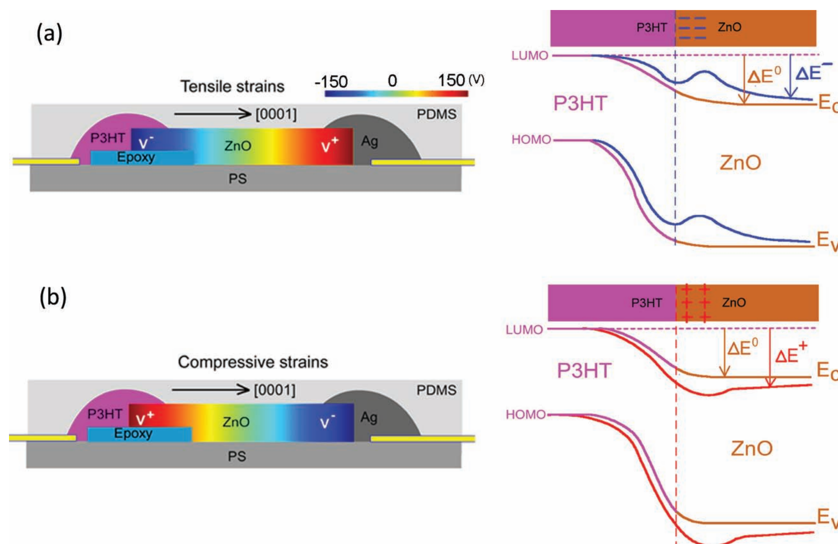

Figure 11. Piezo-phototronic effect on the output of a P3HT/ZnO solar cell. (a) The piezopotential distributions in the stretched device of [0001] type, and the corresponding (b) band diagram of P3HT/ZnO with the presence of negative piezoelectric charges. The blue line indicates the modified energy band diagram by the piezoelectric potential in ZnO. (c, d) Same as in (a, b) but under compressive strain. Reproduced with permission.[33] Copyright ACS, 2011.

distribution, they predicted that the photocurrent of the ferroelectric nanorods can be totally controlled by adjusting its size and states of the polarization "up" and "down". Again, it will be exciting to realize these predicted results experimentally.

5.2. Piezo-Phototronic Effect on Photodetector

The basic principle of a photon detector is based on photoelectric effect, in which the e-h pairs generated by a photon are separated by either a *pn* junction or a SBH. In such a case, the SBH is important for the detection sensitivity of the photon detector. By tuning the SB height in a ZnO wire based UV sensor through applying a strain, we may improve the sensitivity of the UV detector especially when the illumination intensity is rather weak. The responsively of the photodetector is respectively enhanced by 530%, 190%, 9% and 15% upon 4.1 pW, 120.0 pW, 4.1 nW, 180.4 nW UV light illumination onto the wire by introducing a –0.36% compressive strain in the wire (**Figure 12**), which effectively tuned the SB height at the contact by the produced local piezopotential.[7,38] The sensitivity for weak light illumination is especially enhanced by introducing strain, although the strain almost has little effect on the sensitivity to stronger light illumination. Our results show that the piezo-phototronic effect can enhance the detection sensitivity more than fivefold for pW levels light detection.

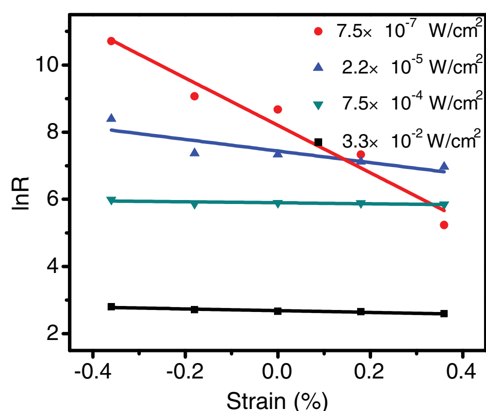

Figure 12. Piezo-phototronic effect on photon detector. Enhancing photon detection sensitivity by piezo-phototronic effect. Responsivity of a ZnO wire UV detector (in units of A/W) as a function of strain under different excitation light intensity on a natural logarithmic scale. Reproduced with permission.[7] Copyright ACS, 2010.

5.3. Piezo-Phototronic Effect on LED

Effective charge recombination is essential for LED. We now show that the piezo-phototronic effect can be used to largely enhance the LED output.[6] Our experiments were carried for a n-ZnO–p-GaN device. A normal force was applied perpendicular to the pn junction interface, which produces a tensile strain along the *c*-axis in the ZnO microwire. At a fixed applied bias above the turn-on voltage (3 V), the current and light emission intensity increased obviously with increase of the compressive strain (**Figures 13**a and 13b). The injection current and output light intensity were largely enhanced by a factor of 4 and 17, respectively, after applying a 0.093% *a*-axis compressive strain, indicating that the conversion efficiency was improved by a factor of 4.25 in reference to that without applying strain. This means that the external true efficiency of the LED can reach ~7.82% after applying a strain, which is comparable to that of the LED structures based on nanorods enhanced hybrid quantum wells LED.

The enhanced LED efficiency is due to piezo-phototronic effect.[6] Under an assumption of no-doping or low-doping in ZnO for simplicity, numerically calculated piezopotential distribution in the ZnO microwire shows (Figure 13c) that a negative potential drop is created along its length when the ZnO microwire is under *a*-axis compressive strain. The finite doping in the wire may partially screen the piezoelectric charges, but it cannot totally eliminate the piezoelectric potential if the doping level is low, thus a dip in the band is possible. The depletion width and internal field may be reduced under this additional component of forward biased voltage. Subsequently, the injection current and emitting light intensity under the same externally applied forward voltage increase when the device is strained.

5.4. Piezo-Phototronic Effect on Electrochemical Processes

Photoelectrochemical (PEC) processes are the fundamental of photon water splitting and energy storages. The key to the PEC efficiency is dictated by the charge generation and

© 2012 WILEY-VCH Verlag GmbH & Co. KGaA, Weinheim

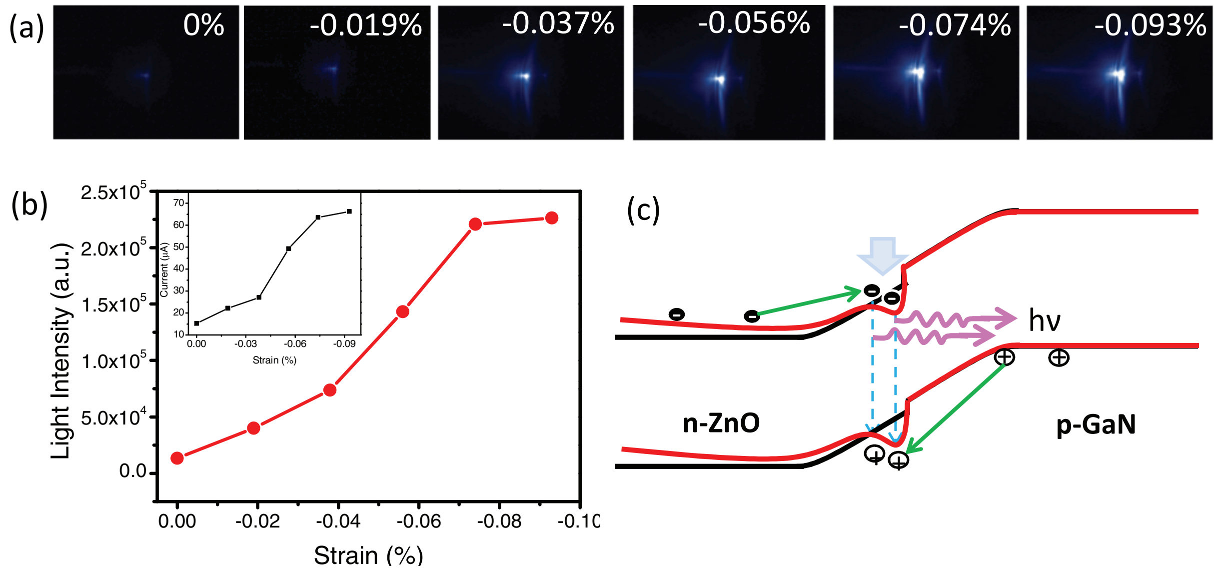

Figure 13. Piezo-phototronic on GaN/ZnO LED. Enhancement of emission light intensity and conversion efficiency of a (n-ZnO wire)-(p-GaN film) LED under applied strain. (a) CCD images recorded from the emitting end of a packaged single wire LED under different applied strain (b) Integrated emission light intensities from the data shown in (b), showing a huge increase in the emission intensity with the increase of the applied compressive strain. The inset is the injection current of the LED at 9 V biasing voltage with the increase of the strain. (c) Schematic energy band diagram of the p-n junction without (upper) and with (lower, red line) applied compressive strain, where the channel created at the interface inside ZnO is due to the piezopotential created by strain. The red dots represent the local piezo-charges near the interface, which produces a carrier trapping channel. The slope of the red line in the lower image at the ZnO side represents the driving effect of piezopotential to the movement of the charge carriers. Reproduced with permission.[6] Copyright ACS, 2011.

separation processes. The basic PEC process can be illustrated in **Figure 14**. The system is made of a n-type semiconductor that is directly interfacing with an electrolyte. The counter electrode is Pt. A natural Schottky barrier of height φ_B is present at the semiconductor-electrolyte interface. Once a photon with an energy higher than the bandgap of the semiconductor shines at the interface, an electron-hole pair is generated. The excited electron tends to drift toward the semiconductor side in the conduction band owing to the inclined band, which then is transported through the external load to the Pt electrode owing to a difference in Fermi level at the two sides. The hole drifts toward the electrolyte. If the energy possessed by the hole is more than the oxidation potential, it can stimulate an oxidation process to cover an A species into A^+. The electron at the Pt side is then recaptured by A^+ if the reduction potential is lower than the Fermi level of Pt, so that it is reduced into A. This is

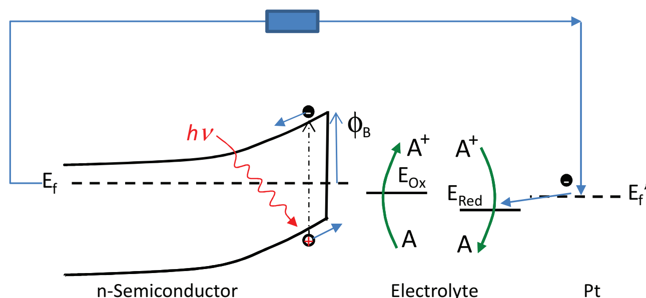

Figure 14. Basic principle of a photoelectrochemical process expressed using band diagram.

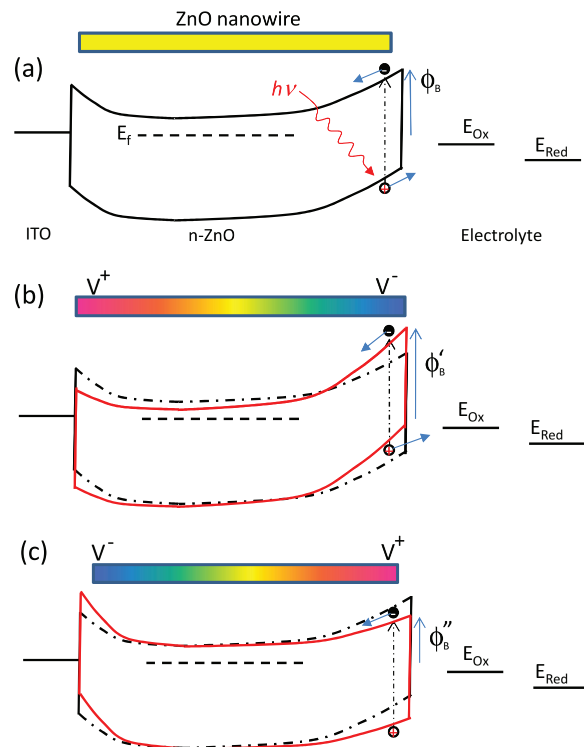

Figure 15. Piezo-phototronic effect on the photoelectrochemical process. (a) Band structure of the PEC with the absence of piezopotential. (b) Band structure of the PEC when the film is under tensile strain so that the side directly interfacing with the electrolyte has a lower piezopotential. (c) Band structure of the PEC when the film is under compressive strain so that the side directly interfacing with the electrolyte has a higher piezopotential.

© 2012 WILEY-VCH Verlag GmbH & Co. KGaA, Weinheim

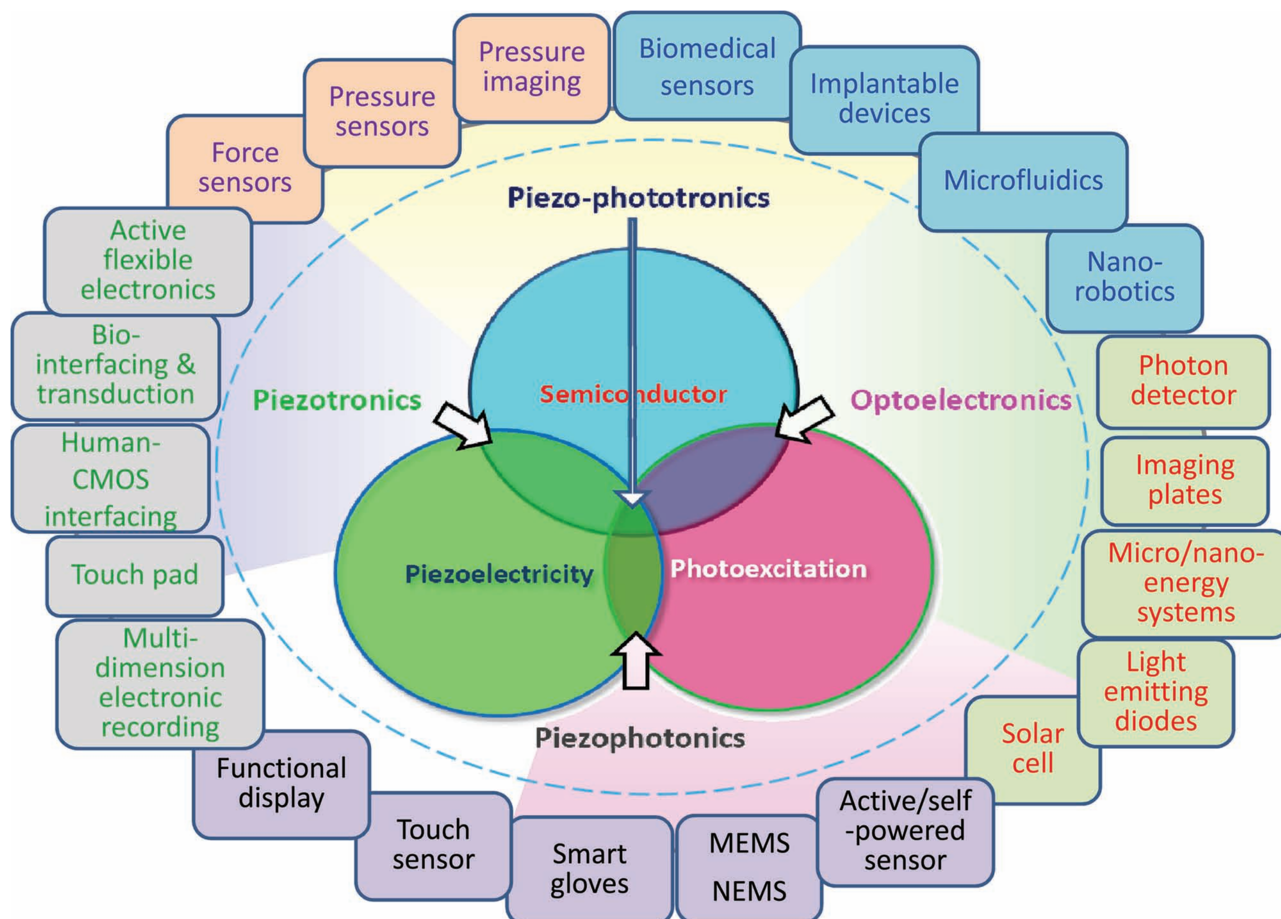

Figure 16. Schematic diagram showing the three-way coupling among piezoelectricity, photoexcitation and semiconductor, which is the basis of piezotronics (piezoelectricity-semiconductor coupling), piezophotonics (piezoelectric-photon excitation coupling), optoelectronics, and piezo-phototronics piezoelectricity-semiconductor-photoexcitation). Potential applications of piezotronics and piezo-phototronics and nanogenerators are projected, which are important future directions and fields in research and applications.

the process of converting photon energy into electricity through a redox process.

For the process shown in Figure 14, the drift of the hole from the semiconductor to the electrolyte will be impossible if the oxidation potential E_{Ox} is significantly higher than the valence band edge of the semiconductor at the solid/liquid interface. In such a case, no charge exchange will be possible, and thus no redox process (**Figure 15**a). For a piezoelectric semiconductor, if a tensile strain is applied to the semiconductor film so that the side directly interfacing with the electrolyte has a lower piezopotential, the valence band edge is lifted up so that it is close to the oxidation potential E_{Ox}, as shown in Figure 15b, the hole has enough energy to trigger the oxidation process. At the same time, the steeply raised conduction band at the electrolyte side accelerates the drift of the electron in the conduction band towards the ITO side. Furthermore, the valence band at the ZnO-ITO contact is lowered, reducing the local resistance or threshold voltage for electron transport. All of these processes are favorable for enhancing the efficiency of PEC.

Alternatively, by switching the strain to a compressive strain in the film, the local piezopotential at the electrolyte interface is high, as shown in Figure 15c, the lowered valance band reduces the energy of the hole so that it may not be effective to stimulate the redox process or at least at a reduced efficiency. Furthermore the flattered conduction band at the electrolyte side reduces the drifting speed of the electron toward the ITO side. The raised conduction band at the ITO side increases the threshold voltage and increases the local resistance. All of these processes can largely reduce the efficiency of PEC. The expected results from Figure 15 has recently been observed by Shi et al.,[39] who showed the strain dependence of the output photocurrent in a ZnO film based PEC solar cell.

5.5. Theory of Piezo-Phototronics

We have developed the theoretical frame of piezo-phototronics by studying the photon emission at the p-n junction and

© 2012 WILEY-VCH Verlag GmbH & Co. KGaA, Weinheim

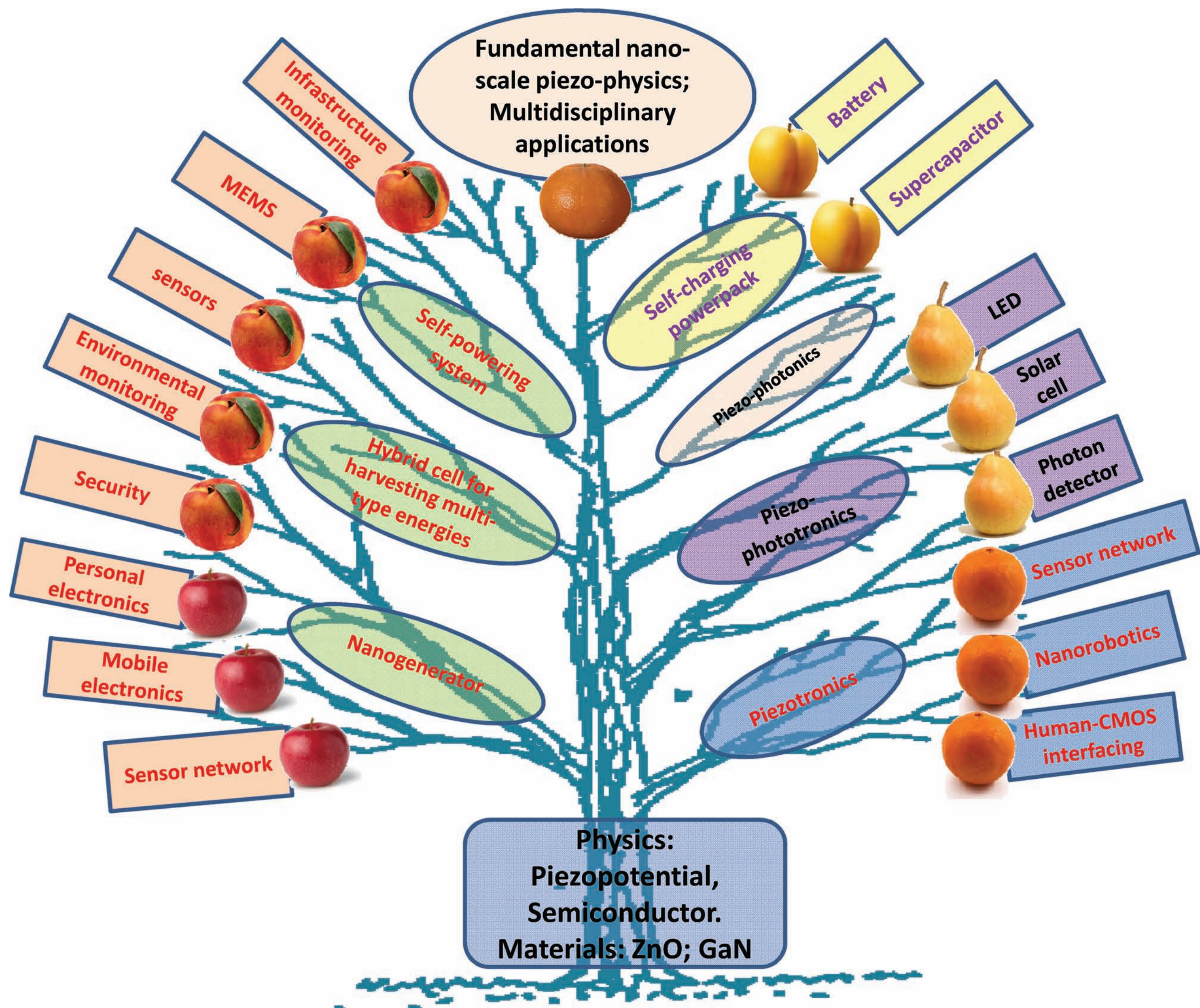

Figure 17. A "tree" idea for summarizing the fields of nanogenerator, hybrid cell for harvesting multi-type energies,[42–45] self-powered system, piezotronics, piezo-phototronics and possibly piezophotonics that have been developed by Wang's group in the last decade. The fundamental "root" of all these fields is: piezopotential and semiconductor as the basic physics, and ZnO as the fundamental materials system. All of the fields are derived based on these basics.

the photon detector in the presence of local piezoelectric charges.[40,41] The analytical results under simplified conditions are derived for understanding the core physics of piezo-phototronic devices, and numerical models are developed for illustrating the photon emission process and carrier transport characteristics of the piezoelectric LED in a practical case. The theoretical results support the experimental data and our physical pictures for the piezo-phototronics. The theory not only establishes the solid physical background of piezo-phototronics, but also provide theoretical support for guiding experimental design.

6. Summary and Outlook

Today's electronics and optoelectronics are mostly based on Si, II–VI and III–V compound semiconductor materials, with a focus on CMOS technology, LEDs, photon detectors, and solar cells. Piezoelectricity, on the other hand, relies on PZT type of perovskite materials, which are not popularly used for electronics and optoelectronics. Owing to the gigantic difference in materials systems, the overlap between piezoelectricity and optoelectronics is rather limited. With the use of wurtzite materials, such as ZnO, GaN and InN, which simultaneously have piezoelectric and semiconductor properties, we have coupled piezoelectricity with optoelectronic excitation processes and coined a few new fields (**Figure 16**).[8] The core relies on piezopotential that is created in a piezoelectric material by applying a stress, and it is generated by the polarization of ions in the crystal. *Piezotronics* is about the devices fabricated using the piezopotential as a "gate" voltage to tune/control charge carrier transport at a contact or junction. *Piezo-phototronic effect* is to use the piezopotential to control the carrier generation, transport, separation and/or recombination for improving the

© 2012 WILEY-VCH Verlag GmbH & Co. KGaA, Weinheim

performance of optoelectronic devices, such as photon detector, solar cell and LED.

We have devoted over twelve years to studying ZnO nanostructures. Our systematic studies and the field coined can be summarized using a "tree" structure, as shown in **Figure 17**. The fundamental "root" of all these fields is: the piezopotential and semiconductor as the basic physics, and the wurtzite structure as the fundamental materials system; the "branches" are the fields we have coined; and the "fruits" are the important applications. Furthermore, fundamental quantum phenomena possibly arising from nanoscale piezo-physics can be explored. It may be possible to use doped PZT perovskite type structures for such studies.

Piezotronics are likely to have important applications in sensors, human-silicon technology interfacing, MEMS, nanorobotics, and active flexible electronics. The role played by piezotronics in interfacing human-CMOS technology is similar to the mechanosensation in physiology. Mechanosensation is a response mechanism to mechanical stimuli. The physiological foundation for the senses of touch, hearing and balance, and pain is the conversion of mechanical stimuli into neuronal signals. We anticipate the near future applications of piezotronics and piezo-phototronics in sensor network, bioscience, human-machine interfacing and integration, and energy sciences.

Acknowledgements

Research was supported by DARPA, Airforce, U.S. Department of Energy, Office of Basic Energy Sciences, Division of Materials Sciences and Engineering under Award DE-FG02-07ER46394, NSF (CMMI 0403671). Thanks to the contributions made by my group members and collaborators to the materials reviewed in this paper, especially to Drs. Jun Zhou, Youfan Hu, Qing Yang, Yan Zhang, Wenzhuo Wu, Ya Yang, Ying Liu, Xudong Wang and Jr-Hau He.

Received: November 14, 2011
Published online: February 14, 2012

[1] http://en.wikipedia.org/wiki/Mechanosensation.
[2] X. D. Wang, J. Zhou, J. H. Song, J. Liu, N. S. Xu, Z. L. Wang, *Nano Lett.* **2006**, *6*, 2768.
[3] J. H. He, C. L. Hsin, J. Liu, L. J. Chen, Z. L. Wang, *Adv. Mater.* **2007**, *19*, 781.
[4] Z. L. Wang, *Adv. Mater.* **2007**, *19*, 889.
[5] Y. F. Hu, Y. L. Chang, P. Fei, R. L. Snyder, Z. L. Wang, *ACS Nano* **2010**, *4*, 1234.
[6] Q. Yang, W. H. Wang, S. Xu, Z. L. Wang, *Nano Letters* **2011**, *11*, 4012.
[7] Q. Yang, X. Guo, W. H. Wang, Y. Zhang, S. Xu, D. H. Lien, Z. L. Wang, *ACS Nano* **2010**, *4*, 6285.
[8] Z. L. Wang, *Nano Today* **2010**, **5**, 540.
[9] Z. L. Wang, J.H. Song, *Science* **2006**, *312*, 242.
[10] Z. L. Wang, *Adv. Funct. Mater.* **2008**, *18*, 3553.
[11] Z. L. Wang, *Mater. Sci. Eng.* **2009**, *R64*, 33.
[12] Z. L. Wang, R. S. Yang, J. Zhou, Y. Qin, C. Xu, Y. F. Hu, S. Xu, *Mater. Sci. Eng.* **2010**, *R70*, 320.
[13] Z. L. Wang, *Nanogenerators for self-powered devices and systems*, Georgia Institute of Technology, SMARTech digital repository, **2011** (http://hdl.handle.net/1853/39262).
[14] Y. F. Gao, Z. L. Wang, *Nano Lett.* **2007**, *7*, 2499.
[15] Z. Y. Gao, J. Zhou, Y. D. Gu, P. Fei, Y. Hao, G. Bao, Z. L. Wang, *J. Appl. Phys.* **2009**, *105*, 113707.
[16] C. L. Sun, J. A. Shi, X. D. Wang, *J. Appl. Phys.* **2010**, *108*, 034309.
[17] Z. Y. Gao, J. Zhou, Y.D. Gu, P. Fei, Yue Hao, G. Bao, Z. L. Wang, *J. Appl. Physics* **2009**, *105*, 113707.
[18] S. S. Lin, J. I. Hong, J. H. Song, Y. Zhu, H. P. He, Z. Xu, Y. G. Wei, Y. Ding, R. L. Snyder, Z. L. Wang, *Nano Lett.* **2009**, *9*, 3877.
[19] L. Vayssieres, *Adv. Mater.* **2003**, *15*, 464.
[20] S. Xu, Z. L. Wang, *Nano Res.* **2011**, *4*, 1013.
[21] Y. G. Wei, W. Z. Wu, R. Guo, D. J. Yuan, S. Das, Z.L. Wang, *Nano Lett.* **2010**, *10*, 3414.
[22] Z. W. Pan, Z. R. Dai, Z. L. Wang, *Science* **2001**, *291*, 1947.
[23] X. D. Wang, C. J. Summers, Z. L. Wang, *Nano Lett.* **2004**, *3*, 423.
[24] Y. Zhang, Y. Liu, Z. L. Wang, *Adv. Mater.* **2011**, *23*, 3004.
[25] P. W. Bridgman, *Phys. Rev.* **1932**, *42*, 858–863.
[26] C. S. Smith, *Phys. Rev.* **1954**, *94*, 42–49.
[27] J. Zhou, P. Fei, Y. D. Gu, W. J. Mai, Y. F. Gao, R. S. Yang, G. Bao, Z. L. Wang, *Nano Lett.* **2008**, *8*, 3973.
[28] W. Z. Wu, Y. G. Wei, Z. L. Wang, *Adv. Mater.* **2010**, *22*, 4711.
[29] X. B. Han, L. Z. Kou, X. L. Lang, J. B. Cia, N. Wang, R. Qin, J. Lu, J. Xu, Z. M. Liao, X. Z. Zhang, X. D. Shan, X. F. Song, J. Y. Gao, W. L. Guo, D.P. Yu, *Adv. Mater.* **2009**, *21*, 4937.
[30] P. Gao, Z. Z. Wang, K. H. Liu, Z. Xu, W. L. Wang, X. D. Bai, E. G. Wang, *J. Mater. Chem.* **2009**, *19*, 1002.
[31] W. Z. Wu, Z. L. Wang, *Nano Letters* **2011**, *11*, 2779.
[32] Y. F. Hu, Y. Zhang, Y. L. Chang, R. L. Snyder, Z. L. Wang, *ACS Nano* **2010**, *4*, 4220; Corrections: **2010**, *4*, 4962.
[33] Y. Yang, W. X. Guo, Y. Zhang, Y. Ding, X. Wang, Z. L. Wang, *Nano Letters* **2011**, *11*, 4812.
[34] J. Grönqvist, N. Søndergaard, F. Boxberg, T. Guhr, S. Åberg, H. Q. Xu, *J. Appl. Phys.* **2009**, *106*, 053508.
[35] N. Søndergaard, Y. He, C. Fan, R. Han, T. Guhr, H. Q. Xu, *J. Vac. Sci. Technol. B* **2009**, *27*, 827–830.
[36] F. Boxberg, N. Søndergaard, H. Q. Xu, *Nano Lett.* **2010**, *10*, 1108–1112.
[37] Y. Zheng, C. H. Woo, *J. Appl. Phys.* **2010**, *107*, 104120.
[38] P. Gao, Z. Z. Wang, K. H. Liu, Z. Xu, W. L. Wang, X. D. Bai, E. G. Wang, *J. Mater. Chem.* **2009**, *19*, 1002.
[39] J. Shi, M. B. Starr, H. Xiang, Y. Hara, M. A. Anderson, J.-H Seo. Z. Ma, X. D. Wang, *Nano Lett.* **2011**, *11*, 5587–5593.
[40] Y. Liu, Q. Yang, Y. Zhang, Z. Y. Yang, Z. L. Wang, *Adv. Mater.* in press.
[41] Y. Zhang, Z. L. Wang, *Adv. Mater.* in press.
[42] C. Xu, X. D. Wang, Z. L. Wang, *J. Am. Chem. Soc.* **2009**, *131*, 5866.
[43] B. J. Hansen, Y. Liu, R. S. Yang, Z. L. Wang, *ACS Nano* **2010**, *4*, 3647.
[44] D. Choi, M. J. Jin, K. Y. Lee, I. S.-G. S. Yun, X. Bulliard, W. Choi, S. Y. Lee, S.-W. Kim, J.-Y. Choi, J. M. Kim, Z. L. Wang, *Energy Environ. Sci.* **2011**, *4*, 4607.
[45] C. F. Pan, Z. T. Li, W. X. Guo, J. Zhu, Z. L. Wang, *Angew Chem. Int. Ed.* **2011**, *50*, 11192

© 2012 WILEY-VCH Verlag GmbH & Co. KGaA, Weinheim